

RESEARCH ARTICLE

A study on the design and performance analysis of an air-cooled waste heat recovery system for use in motorcycle engines

Haluk Güneş^{*1}, Mehmet Akif Kunt¹¹Kütahya Dumlupınar University, Tavşanlı Vocational School, Department of Motor Vehicles and Transportation Technologies, Automotive Programme, Kütahya, Türkiye

Article Info

Article history:

Received 05.05.2022

Revised: 28.06.2022

Accepted: 29.06.2022

Published Online: 30.06.2022

Keywords:

Motorcycle engine

Internal combustion engine

Thermoelectric generator

Waste heat recovery system

Heat transfer

Abstract

In this study, a waste heat recovery system (WHRES) design with a heat exchanger inside to generate electricity from the exhaust gas heat energy discharged from a single-cylinder gasoline motorcycle engine using a thermoelectric generator (TEG) and system performance measurements were made. It was desired that the WHRES should not interfere with the flow of exhaust gas and be easily mounted on any engine. Measurements of the electricity generation performance of the system and the temperature distributions on the hot and cold surfaces of the TEGs were made. In addition, the simulations of the system with Ansysy Fluent software were made and the test results and measurements were compared. Images were taken with a thermal camera to verify the temperature values measured during the experiments. A total of 6 TEGs, 3 above and 3 below, are placed on the heat exchanger symmetrically. The results were recorded during the engine's maximum power cycle of 5500 1 / min. Under this condition, 2W electrical power was obtained from TEGs at 30 ohm load resistance. The obtained waste heat recovery power can be used both for operating the LED warning lamps in the vehicles and for charging some mobile devices from USB. The 371 K temperature measured on the cold surface of the TEGs yielded similar results with the 374 K temperature recorded by thermal cameras and obtained by simulation. There is a difference of 20 K between the hottest region and the coldest region on the cold surfaces of TEGs. Due to this difference, the electricity generation performance of TEGs decreases. This temperature difference can be reduced with changes to the WHRES design.

1. Introduction

Studies made on recycling of wastes have come to prominence in every field in recent years [1,2]. Especially the increase in studies related to waste energy recovery in automobiles indicates that such issue will become more important in the future [3, 5]. Internal combustion engines (ICE) used in automobiles are defined as engines transforming thermal energy into motion energy [6]. In this context, during energy transformation, a certain amount of thermal energy becomes waste without being transformed into useful work due to efficiency of ICEs. When thermal efficiency of ICEs is considered as 30%, approximately 35% of remaining waste thermal energy is thrown out by means of exhaust system, and 35% is thrown out by means of cooling and lubrication system [7]. Electricity can be generated via thermoelectric generators (TEGs) by using the thermal energy thrown out from the exhaust system. In their study, Ding Lou et al. have placed different heat exchangers, which have an inclination angle between 0° and 30°, at the outlet of exhaust gas. [8]. There are four fins inside such heat exchangers in order for better distribution of heat during conduction of exhaust gas. There are two groups of TEG on the heat exchanger, which are placed opposite to each other and each of which includes four items. Cold surface of TEGs is cooled by means of water. The inclination angle decreases the temperature difference between the uppermost TEG and

hindmost TEG. As a result, it has been observed that as the inclination angle increases, the power generated in TEGs increases too.

Massaguer et al. have placed TEG at the exhaust gas outlet of automobiles, which they call ATEG [9]. In that study, they have focused on gaining the highest output power by means of a small system and they have obtained experimental results depending upon various engine speed values. On invariant conditions, maximum power output was obtained as 5.52 W at 15% acceleration and 2000 rpm, and as 111.22 W at 85% acceleration and 2000 rpm. Temporary tests have shown that the method of driving the vehicle is one of the important factors affecting ATEG performance for waste heat recovery.

Wang et al. have compared cylindrical heat exchangers according to two different fin structures having twisted and spiral fins inside the exhaust system [10]. For both situations, modelling has been made by means of computational fluid dynamics and the results have been evaluated. For heat exchangers with twisted fin, calculations have been made for fin angle (0°, 5°, 10°, 15°, 20°), fin thickness (0.001m, 0.002m, 0.003m, 0.004m and 0.005m) and wing height 0.035m, 0.040m, 0.045, 0.050m and 0.055m). For heat exchangers with spiral fin, calculations were made for spiral step (0.015m, 0.030m, 0.045m, 0.060m and 0.075m), spiral fin thickness (0.001m, 0.002m, 0.003m, 0.004m and 0.005m) and fin height (0.030m,

Corresponding Author: Haluk GÜNEŞ
E-mail: haluk.gunes@dpu.edu.tr

How to cite this article:

Güneş, H., and Kunt, M. A., A Study on the Design and Performance Analysis of an Air-Cooled Waste Heat Recovery System for Use in Motorcycle Engines, The International Journal of Materials and Engineering Technology (TIJMET), 2022, 5(1): 53-60

0.035m, 0.040m, 0.045m and 0.050m). As a result, it has been observed for heat exchanger with twisted fin that wall temperature of the heat exchanger increases as the fin thickness increases, change of temperature of heat exchanger cannot be determined clearly as the inclination angle increases, and the temperature increases. For heat exchanger with spiral fin, it has been observed that the heat increases at the beginning, it starts to decrease as the fin thickness increases, it decreases as the fin thickness increases and it increases as the fin height increases.

Hsu et al. have designed a system, in which 24 TEGs are placed in the middle part of the exhaust pipe of the automobiles [11]. They have determined open circuit voltage and maximum power output of the system as a function of the temperature difference. Moreover, they have tried to put forward the power generated by a commercial TEG module by supporting the system with simulations and experiments. In their study, they have carried out the cooling process by means of aluminium heat exchanger, copper cooler and fans above them. They have determined ambient air temperature as 300K and exhaust gas temperature as 573K, which are boundary conditions. As a result, it has been observed that there was 30K temperature difference between cold surface and hot surface, and they have obtained an output power of 12.41 W at engine speed of 3500 rpm and load resistance of 30 ohm.

Temizer et al. have placed an ATEG system including a single-cylinder ICE and 20 TEGs [12]. During their study, they have made experiments at engine speeds of 1250, 1750 ve 2250 rpm respectively, and they have found the electrical energy they generated as 7.36W, 21.52W and 32.8W respectively. At the same time, they have made simulations of the experiments by CFD software and they have compared the results.

He et al. have designed a system for exhaust systems of automobiles and developed cooling experiments and mathematical method for four different cooling states [13]. They have studied on flow of refrigerant in the same and opposite direction with the exhaust gas for air and water-cooling systems. As a result, they have observed that the refrigerant flowing in the same direction with the exhaust gas has better cooling condition and such condition has highly positive effect on the power generated in TEGs.

Cho et al. have made a study related to cooling of TEGs [14]. They have chosen aluminium as coolant and they have used two systems in order to eliminate the heat, a side-fan called SMF and a top-fan called TMF; and they have compared such two systems. They have supported their study with CFD software. While they have used a single fan separately for TEGs from one to five with SMF, they have used one fan for each TEG from one to five with TMF. In TMF system, which has more fans, the fans with three TEGs have been rotated at 8000 rpm, and the fans with four and five TEGs have been rotated at 7000 rpm. In SMF system, which only has a single fan, the fan have been rotated respectively by 8000, 11000, 12000, 13000, 14000 and 15000 rpm from the system with one TEG to the one with five TEGs. When such five states have been compared, it has been seen in terms of the total generated net power that SMF system was much more efficient in the system with one to three TEGs, and the efficiency decreased in the system with four and five TEGs.

In one of his studies, Kunt have measured performance of TEGs, which is depending on external load resistance [15]. In this line, it has been stated that as the load resistance increases, output voltage increases but the current decreases. During his experiments, he has reached to 250°C as maximum temperature

and determined the temperature difference between surfaces as 40°C. In terms of external load resistance, he has made experiments at 5, 10, 15, 20, 35, 35, 40, 45Ω, and he has compared the results with the calculations.

Khail et al. have used TEGs in order to benefit from the thermal energy of hot flue gases [16]. In their study, they have placed heat dissipater plates into the hot parts of the TEGs for better dissipation of heat, and for cooling process they have used separate finned cooler for each TEG. In front parts of finned coolers which are located in the direction of air flow, non-conductive plates, deflecting the air at various heights, have been placed and individual simulations have been made for each of them.

Deflection plates have a depth of 14mm, 20mm, 30mm and 50mm respectively. Moreover, they have made an experiment without deflection plate and compared it in terms of the power generated in the TEGs. As a result, in coolers without plate, the foremost cooler attracted much more heat; and at 50mm which is the deepest plate, the coolers had thermal diffusivity close to each other and they conducted more heat. It has been observed in terms of the power generated in TEGs that coolers with a depth of 50mm are 126% more efficient than the ones which are classical, conductive and do not have plate. There are studies in which thermoelectric materials are used as coolers [17, 18].

2. Thermoelectricity and thermoelectric generators

Thermoelectric generators function on the basis of generating electricity by benefiting from the temperature difference at semi-conductors. In their internal structure, P and N-type semi-conductors are arrayed sequentially and combined serially by copper from top parts. Upper and lower sides of the TEGs are covered by ceramic. They have the principle of generating electricity depending upon the temperature difference between upper and lower surfaces. In Figure 1, structure of semi-conductors of TEGs is shown. In this structure, when one side is heated and the other side is cooled, the module starts to generate electricity.

In order to generate electricity in TEGs, three basic principles, which are Seebeck Effect, Peltier Effect and Thomson Effect, should be taken into consideration [20]. Seebeck Effect can be explained as generating electricity current from temperature difference and is expressed by the general equation in Equation 1 [21].

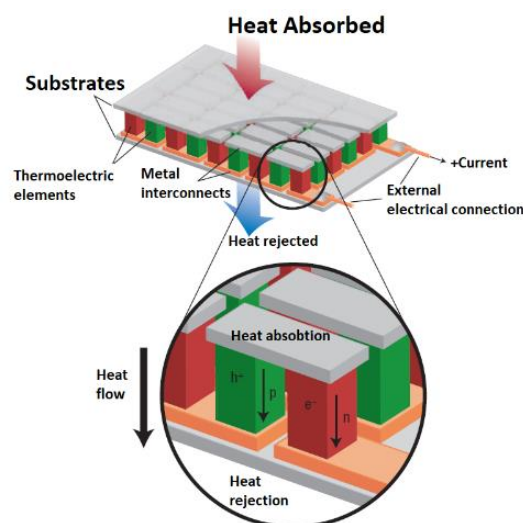


Figure 1. Internal structure of TEG showing the direction of charging flow during power generation [19]

In this equation, U refers to the potential difference, α_{AB} refers to the Seebeck coefficient difference between the material A and B, and ∇T refers to the temperature difference between hot and cold surfaces. Peltier Effect explains the principle asserting that the heat is absorbed from one of the connection points of conductors A and B, which are different from each other, and the heat is diffused from the other connection point [22].

$$\alpha_{AB} = V/\nabla T \quad (1)$$

In Equation 2, π_{AB} refers to the Peltier coefficient, I refers to the current applied, and $Q_{peltier}$ refers to the heat conducted. Thomson Effect is a negligible magnitude and defined as the heating degree per unit length, and expressed by Equation 3 [22].

$$\pi_{AB} = Q_{peltier}/I \quad (2)$$

$$Q_{thomson} = -\tau_{AB}I\nabla T \quad (3)$$

In Equation 3, τ refers to the Thomson coefficient and $Q_{thomson}$ refers to the Thomson heat absorbed or released within the wire. While generating electricity in TEGs, it should be loaded by a load resistance. When such load resistance is close or equal to the internal resistance of TEG, the current and power generated increase evenly [23, 24]. In the experiments, RC 12-8 L model Single-Stage Thermoelectric Module, produced by Marlow Industries Company, has been used.

3. Materials and methods

In this study, it has been aimed to generate electricity from waste exhaust gas heat by benefiting from TEGs in motorcycles

and stationary unit engines. In order to support the experiments, the issues of modelling heat exchanger via Fluent software and heat have been handled. Accuracy of our study has been tested by comparing the results of experiments and the results of simulations. Technical specification of the engine used during the experiments is shown in Table 1.

Table 1. Technical specification of the test engine

| | |
|----------------------------|----------|
| Engine Volume | 49cc |
| Engine Power | 1.5 Hp |
| Number of cylinders | 1 |
| Number of stroke | 2 stroke |
| Cylinder diameter | 42.50 mm |
| Stroke length | 34.54 mm |
| Intake and exhaust process | Port |
| Cooling system | Air |

The experiments have been carried out at load speeds and at a throttle opening of $\frac{3}{4}$. Engine speed has been accelerated up to 6500 rpm and loading has been made at 500 rpm intervals consecutively. At that point, torque and power values of the engine, speed and temperature of the exhaust gas entering into and exiting from the heat exchanger, and temperatures of TEGs at hot surfaces have been recorded. Thanks to such values, boundary conditions for simulations have been determined in Fluent software, and the values obtained by experiments and the results of the simulations have been compared. At the same time, temperatures occurring on surfaces at each speed option have been monitored by thermal camera and critical points have been photographed. In Figure 2a, experiment mechanism is shown.

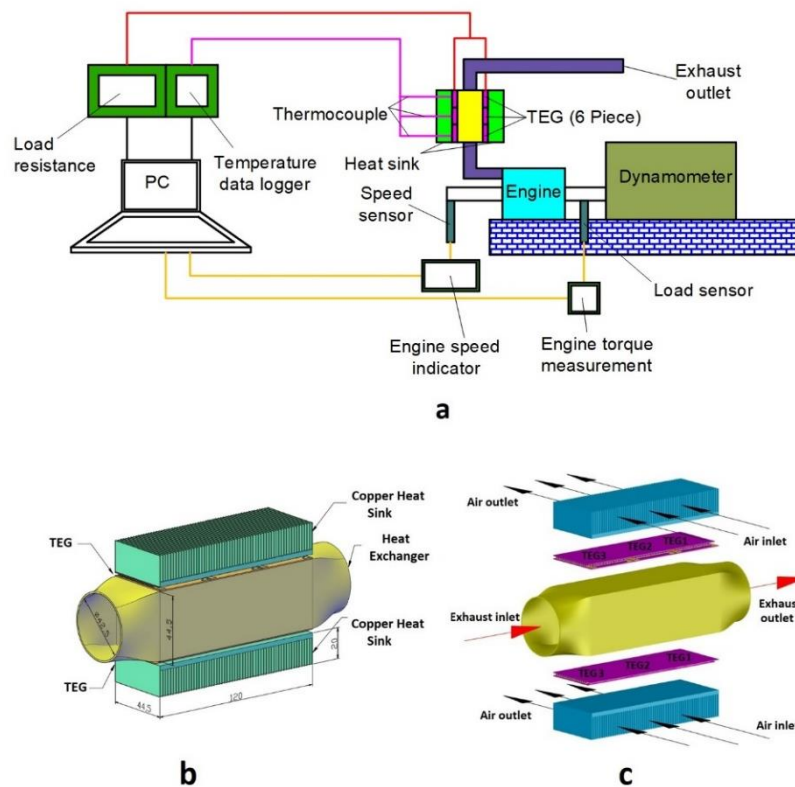


Figure 2. (a) Appearance of experiment mechanism, (b) Connections and size of heat exchangers, (c) installation of heat exchangers and TEGs

A heat exchanger has been connected to the exhaust outlet of the test engine, and 6 TEGs have been used in total, 3 of which are located in the upper part of the heat exchanger and 3 of which are located in the lower part. The heat exchanger has a square structure. In Figure 2-b, drawing and size of TEGs are shown.

The heat exchanger has been produced from 1050 steel having a thickness of 2mm. In coolers, copper material has been preferred due to the fact that heat conduction coefficient of copper is more than aluminium. In Figure 2-c, installation of the heat exchangers and TEGs are shown. The engine we used for the experiment is a stationary engine; for cooling process, the air flow is provided by means of the fan in the direction shown

in Figure 2-c and accordingly the cooling fins have been placed towards such direction. In Table 2, thermo-physical properties of the exhaust gas, calculated at temperatures obtained according to load engine speeds during experiments, have been given [25].

Apart from fluids, since copper is used in the cooler, steel in the heat exchanger, ceramics and semiconductors are used in TEG, their thermo-physical properties must also be introduced to the system. For this purpose, the information in Table 3 was used. Since Bismuth Telluride (Bi_2Te_3) is generally used in P and N semiconductors, the thermo-physical properties of such materials are preferred.

Table 2. Thermo-physical properties of exhaust gases entering into the heat exchanger

| Thermo-physical properties of exhaust gas entering the heat exchanger | | | | |
|---|-------------------------|-------------------|---------------|-----------------------------|
| Engine speed | Exhaust gas temperature | Density | Specific heat | Heat conduction coefficient |
| <i>rpm</i> | <i>T</i> | ρ | c_p | $k \cdot 10^3$ |
| 1/min | K | kg/m ³ | J/kgK | W/mK |
| 4000 | 491 | 0.74 | 1128.75 | 36.50 |
| 4500 | 527 | 0.68 | 1138.04 | 38.97 |
| 5000 | 579 | 0.63 | 1153.10 | 42.18 |
| 5500 | 600 | 0.61 | 1160.12 | 43.64 |
| 6000 | 623 | 0.58 | 1166.96 | 45.27 |

Table 3. Specification of solid materials composing the parts

| Part | Material | Density | Specific Heat | Thermal Conductivity |
|--------------------|-------------------|-----------------------------|----------------|----------------------|
| | | ρ Kg/m ³ | C_p J/kgK | K W/mK |
| TEG | | | | |
| Insulation plates | Alumina | 3720 | 837.36 | 35.3 |
| Semi-conductor | Bismuth Telluride | 7700 | 544.28 | 1.5 |
| Electric conductor | Copper | 8978 | 381 | 387.6 |
| Heat exchanger | Steel | 8030 | 502.48 | 16.27 |
| Heat sink | Copper | 8978 | 381 | 387.6 |

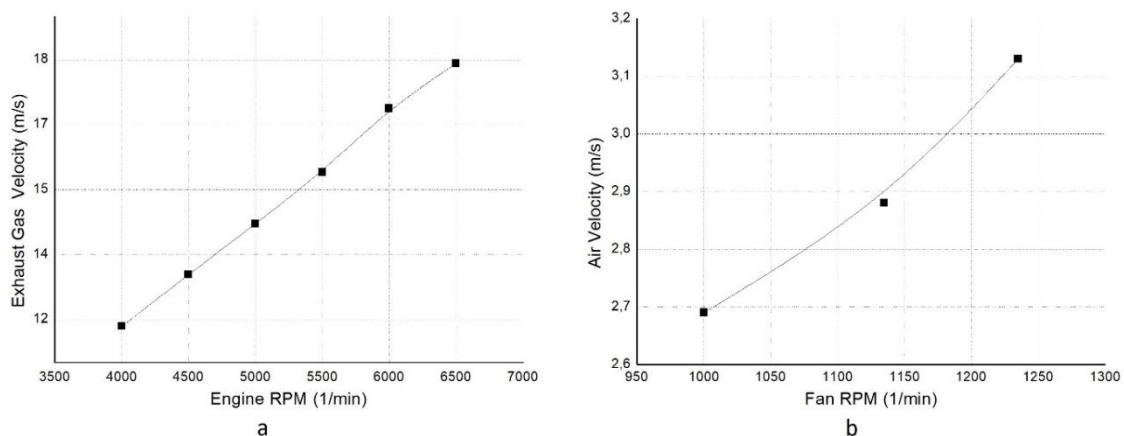


Figure 3. (a) Exhaust gas velocity according to engine speed, (b) air velocity according to fan speed

Air is provided to the cooling fins by means of a fan. In the simulation, the velocity of that air has been identified as boundary condition for air velocity entrance. Velocity of exhaust gas has been identified as boundary condition for velocity entrance of gases entering into the heat exchanger. During simulations, properties at 600 K temperature belonging

to the state of 5500 1/min engine speed on constant functioning conditions have been used. In Figure 3-a, air velocity measured according to fan speed, and in Figure 3-b, exhaust gas velocity measured according to engine speed, have been given

4. Mesh Structure and boundary conditions

As outlet of the exhaust gas and outlet of air from the cooling area are towards the atmosphere in the simulation, pressure has been introduced as boundary condition. In simulations made by Fluent software, the system should be designed as three-dimensional, mesh structure should be formed and finally calculations should be started. The computer system to be used in mesh structure and calculations should have dual processor multi-core structure and high capacity RAM hardware. In such kind of calculations or image processing programmes, GPU (Graphics Processing Unit) hardware accelerates the transactions [26].

The geometer has been simplified as much as possible in order to make the programme accelerate the transaction, and design mode and symmetry properties have been used. As such process creates less mesh and node point, a much more rapid solution has been provided.

When the quality and properties of the mesh structure are examined, 12406390 elements and 17644993 nodes were formed. The min orthogonal quality was 0.10 and the max aspect ratio was 27.78. In boundary layer, longer peripheries have been created towards the direction of flow. This situation has increased Aspect Ratio. Aspect Ratio is defined as the ratio of long peripheries of three-dimensional mesh elements to the short peripheries. Orthogonal quality is a quality-related property indicated between zero and one; as it gets closer to 1, the quality increases.

In order to determine type and model of flow for simulation, Reynolds number should be found for both air and exhaust gas. To this end, Equation 4 has been used.

$$Re = \frac{\rho \cdot V_m \cdot D}{\mu} \quad (4)$$

Here, $\rho = 0.61 \text{ kg/m}^3$ refers to the density of exhaust gas, $V_m = 15.4 \text{ m/s}$ refers to speed of exhaust gas while entering into the heat exchanger, $\mu = 279.19 \text{ Ns} \cdot 10^{-7}/\text{m}^2$ refers to its dynamic viscosity, $D = 0.0425 \text{ m}$ refers to entrance diameter of the heat exchanger. Reynolds number has been found as 13663 according to such values; and as $Re \geq 2300$, exhaust flow is in turbulent area. The cooling air enters into the system from a square structure. While calculating Reynolds number for air, we have to find dynamic diameter from such section. Accordingly, such diameter turns into D_h and can be calculated by Equation 5.

$$D_h = \frac{4 \cdot A_c}{P} = \frac{2 \cdot a \cdot b}{2 \cdot (a+b)} \quad (5)$$

Here, $a=0.16$ and $b=0.06$ are lengths of the peripheries of square section, and hydraulic diameter is found by $D_h = 0.0872 \text{ m}$. When measured velocity of air has been derived as $\rho = 1.16 \text{ kg/m}^3$, $\mu = 184.6 \text{ Ns} \cdot 10^{-7}/\text{m}^2$ and $V_m = 3.13 \text{ m/s}$ from table related to thermo-physical properties of air, Reynolds number has been found as 17171. As $Re \geq 2300$, the flow is in turbulent area. Realizable method has been chosen from k- ϵ turbulence model, which gives more real-like results and frequently used.

The heat transfer solution on hot and cold ceramic surfaces is solved by the equation given in Equation 6 [27].

$$\rho c \frac{\partial T}{\partial t} = \frac{\partial}{\partial x} \left(k \frac{\partial T}{\partial x} \right) \quad (6)$$

Equation 7 was used in the energy balance analysis in TEGs [27].

$$\rho c \frac{\partial T}{\partial t} = \frac{\partial}{\partial x} \left(k \frac{\partial T}{\partial x} \right) + \frac{J^2}{\sigma} - \tau J \frac{\partial T}{\partial x} \quad (7)$$

Here, $k (\text{Wm}^{-1} \text{K}^{-1})$ is the thermal conductivity coefficient, $\sigma (\text{S m}^{-1})$ is the electrical conductivity coefficient, $\tau (\text{V K}^{-1})$ is the Thomson coefficient and $J (\text{A m}^{-2})$ is the current density. The Nusselt number can be found by Equation 8 [27].

$$Nu = \frac{(0.5f)(Re-1000)Pr}{1+12.7(0.5f)^{1/2}(Pr^{2/3}-1)} \quad (8)$$

Here, f refers to friction factor. A single correlation, developed by Petugov on smooth surfaces and covering a wide range of Reynolds number, is given in Equation 9 [27].

$$f = A + B/Re^{1/m} \quad (9)$$

5. Results and discussion

Results obtained with relation to exhaust gas velocity is given in Figure 4-a. A deceleration has occurred in exhaust gas velocity as an expansion has happened inside the heat exchanger. At the same time, a lower profile has emerged in areas, which are closer to the surface of heat exchanger, when compared to the middle sections.

In Figure 4-b, temperature depending on the flow on cold surfaces is shown. As it can be understood, the hottest points in TEGs occur at the inlet of the exhaust gas. The highest temperature occurring in TEG is 381K. Such kind of temperature values has been determined during the experiments. The temperature difference between the hottest and coldest surfaces is 14K. Such situation indicates that each TEG will show different performance during electricity generation.

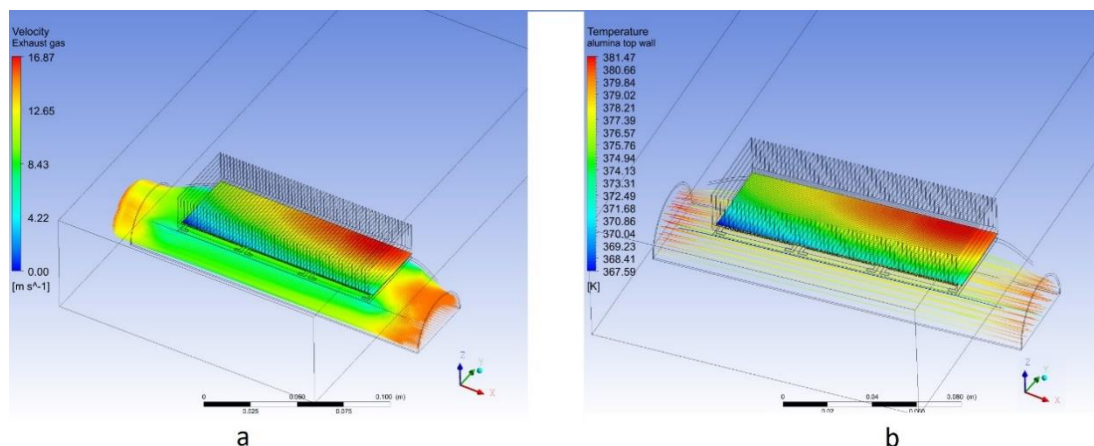


Figure 4. Distribution of temperature on hot surfaces of TEGs depending on flow.

Temperatures measured during the experiments are given in Figure 5-a. In this figure, temperatures of the exhaust gas, entering into and exiting from the heat exchanger, and the temperatures measured on cold surfaces of each TEG are given. TEG3 is the module closer to the exhaust gas inlet, TEG2 is the middle one and TEG1 is the one closer to the exhaust gas outlet respectively. When temperatures measured on cold surfaces of

TEGs have been examined, it has been seen that they are compatible with the temperature values given in Figure 4-b. However, measurements are the values derived from the middle section of cold surfaces of TEGs. Accordingly, it gives the temperature of a single point. However, distribution of temperature obtained from the simulation shows a wider range of and detailed temperature value.

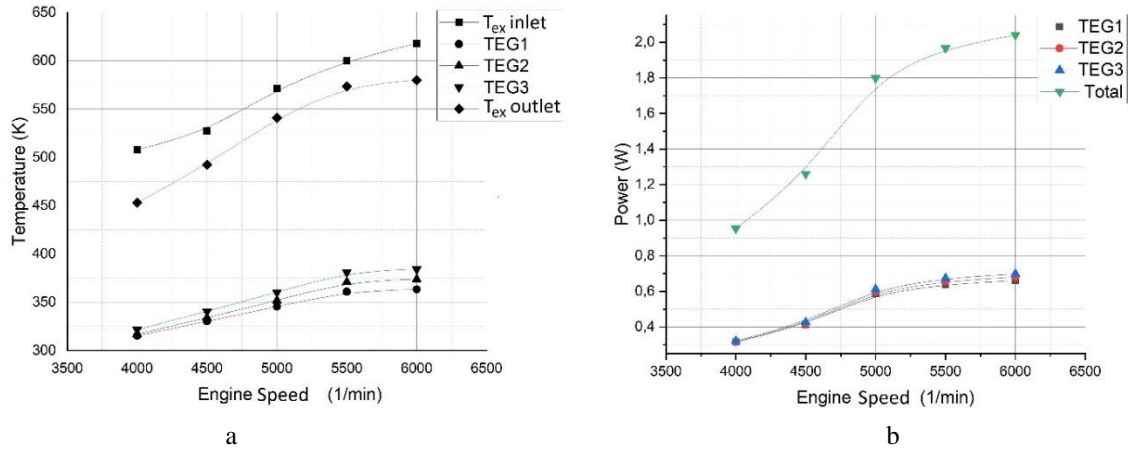


Figure 5. (a) Inlet and outlet of heat exchanger according to engine speed and temperature value measured on cold surfaces of TEGs, (b) electrical power values generated in TEGs and in total depending on engine speed

As can be seen from this graph, more temperature has occurred on the cold surfaces of the TEGs close to the inlet of the exhaust gas. A similar situation has been observed in the simulations. Such kind of a result affects the electricity generation performance in TEGs. In Figure 5-b, measurements of electrical power generated in each TEGs and in total are given. Difference in temperatures results in difference in electrical power generated in TEGs. In order to eliminate such differences and to provide equal distribution of temperature, changes can be made in the heat exchanger. Accordingly, the power, which is 2W at maximum, can be increased.

simulations is 381K. In Figure 6-b, there is an evaluation of the state related to temperature distribution of heated air and the cooler. Here, the distribution of temperature created by the air exiting from the cooler on the bottom within the control volume after taking the temperature on. At the same time, when distribution of temperature on cooler surface is examined, it has been observed that a difference of 20K occurs between the hottest and the coldest parts.

In Figure 6-a, photo taken by thermal camera at engine load 5500 1/min speed is seen. Thermal camera is an 880 model of Testo company. Temperatures measured here show similarity to the results of simulation. Especially, while the hottest point on the cooler is 386K, the highest temperature occurred during the

In Figure 7, the comparison of the temperatures measured on the cold surfaces of TEGs with those calculated in simulations is given. In both cases, it is seen that the temperatures are close to each other. It is normal for temperatures to decrease towards the exhaust gas outlet. However, the temperatures of TEGs being as close to each other as possible will increase the total electrical energy to be produced.

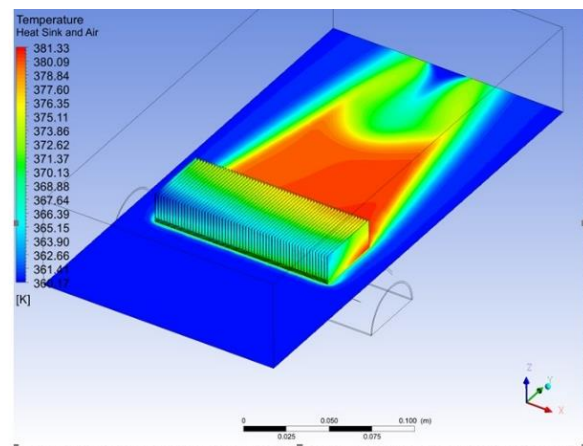
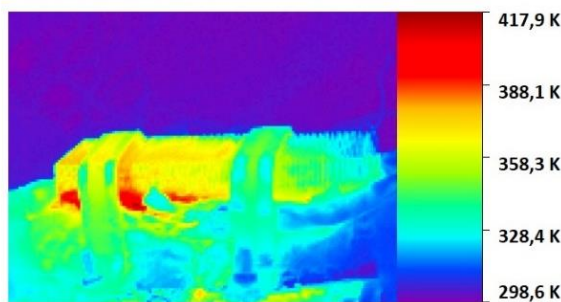


Figure 6. (a) Photo taken by thermal camera at load engine speed of 5500 1/min, (b) Distribution of temperature in the cooler and air control volume

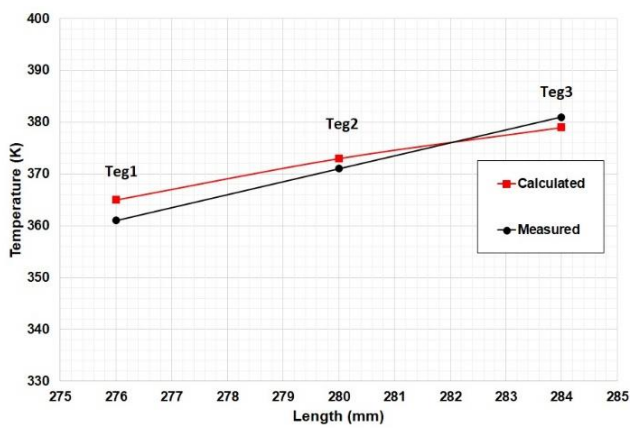


Figure 7. Comparison of measured and calculated temperatures on cold surfaces of TEGs

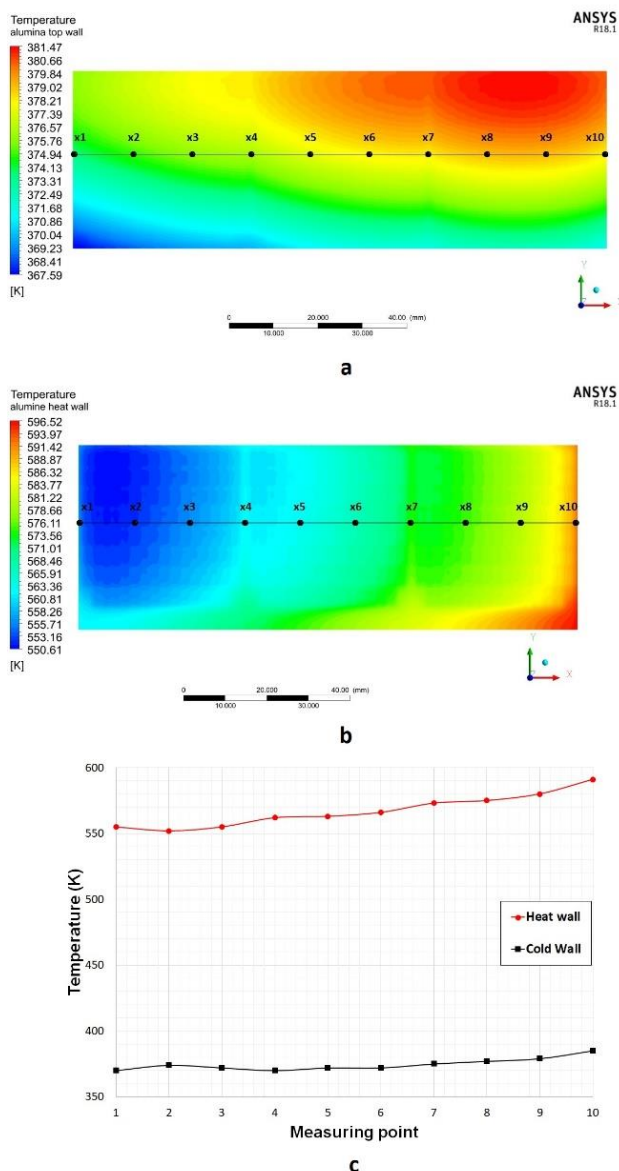


Figure 8. (a) Heat wall surface, (b) cold wall surface, (c) comparison of the calculated temperatures on the cold and hot surfaces of TEGs

Figure 8 shows the comparison of the temperatures calculated on the hot and cold surfaces of the TEGs. Two

significant issues are worth considering here. First one of them is the temperature difference between the hot surface and cold surface of TEG, which is 226K. However, such value is the highest temperature difference. The second one includes the highest and lowest temperatures on hot surface, which depends on cooling of the exhaust gas entering into the heat exchanger towards the outlet.

6. Conclusions

In this study, temperature differences, occurring in the heat exchanger during generation of electricity by using waste exhaust gas heat of a single-cylinder gasoline engine, have been researched. For electricity generation, six TEGs have been placed in total, three of which on the upper part and three of which on the lower part of the heat exchanger. Measurements of temperature values occurring on them and the results of simulations have been compared. Fan air has been used for cooling the TEGs. Calculations made at the end of the experiments and by Fluent software have been compared with each other. As a result, a significant similarity has been observed in values. However, measured temperature values are from the centre of TEGs and from a single point. On the other hand, in the simulation, temperature values on a wider surface can be put forward. During the experiments, images have been taken by thermal camera in order to support the measurement values. Hence, temperature differences that can occur in TEGs have been observed, and it has been put forward that performance changes can occur in electricity generation. Here, 2W power was produced at a constant motor speed of 5500 1/min by using six TEGs. The power produced can be increased by increasing the number of TEGs. With this electricity to be produced from waste heat in small-volume engines such as motorcycle engines, various mobile devices are charged. It is also used in the operation of warning led lamps in these electric vehicles. In follow-up study, changes on heat exchanger and equal distribution of temperatures can be examined. Thus, the total power obtained from the six TEGs can be increased.

Author Contributions

Haluk Güneş: Testing, Writing-original draft

Mehmet Akif Kunt: Supervision, review & editing

References

- Dong, H., Geng, Y., Yu, X., Li, J., Uncovering energy saving and carbon reduction potential from recycling wastes, *Journal of Cleaner Production*, **2018**, 205: 27-35
- Khoo, H.H., LCA of plastic waste recovery into recycled materials, energy and fuels in Singapore. Elsevier Resources, Conservation & Recycling, **2019**, 145: 67-77
- Arias, D.A., Shedd, T.A., Jester RK. Theoretical analysis of waste heat recovery from combustion engine in a hybrid, *SAE Transactions*, **2006**, 115: 777-784.
- Yasa, T., Thermodynamic evaluation of energy recovery system for heavy duty diesel engine by using organic rankine cycle, *Anadolu University Journal of Science and Technology A Applied Sciences and Engineering*, **2017**, 18: 573-583

5. Kunt, M.A., İçten yanmalı motor atık ısılarının geri kazanımında termoelektrik jeneratörlerin kullanımı, *El-Cezeri Journal of Science and Engineering*, **2016**, 3: 192-203
6. Stone, R., *Introduction to Internal Combustion Engines*, London: The Macmillan Press. **1992**
7. Galindo, J., Serrano, J.R., Dolz, V., Kleut, P., Brayton cycle for internal combustion engine exhaust gas waste heat recovery, *Advances in Mechanical Engineering*, **2015**, 7: 1-9
8. Lou, D., Wang, R., Yu, W., Sun, Z., Meng, X., Modelling and simulation study of a converging thermoelectric generator for engine waste heat recovery, *Elsevier Applied Thermal Engineering*, **2019**, 153: 837-847
9. Massaguer, A., Massaguer, E., Comamala, M., Pujol, T., Montoro, L., Cardenas, M.D., Carbonell, D., Bueno, A.J., Transient behavior under a normalized driving cycle of an automotive thermoelectric generator, *Elsevier Applied Energy*, **2017**, 206: 1282-1296
10. Wang, T., Shaolei, M.A., Teg heat performance study about improved fin structures, *Thermal Science International Scientific Journal*, **2018**, 22: 101-112
11. Hsu, C.T., Huang, G.Y., Chu, H.S., Yu, B., Yao, D.J., Experiments and simulations on low-temperature waste heat harvesting system by thermoelectric power generators, *Elsevier Applied Energy*, **2011**, 88: 1291-1297
12. Temizer, I., Yuksel, T., Can, I., Alnak, D.E., Analysis of an automotive thermoelectric generator on a gasoline engine, *Thermal Science International Scientific Journal*, **2020**, 24: 137-145
13. He, W., Wang, S., Lu, C., Zhang, X., Li, Yanzhe., Influence of different cooling methods on thermoelectric performance of an engine exhaust gas waste heat recovery system, *Elsevier Applied Energy*, **2016**, 162: 1251-1258
14. Cho, Y.H., Park, J., Chang, N., Kim, J., Comparison of cooling methods for a thermoelectric generator with forced convection, *Energies*, **2020**, 13: 3185-3204
15. Kunt, M.A., An experimental investigation of exhaust waste heat recycling by thermoelectric generators under different thermal conditions for internal combustion engines, *Proc IMechE Part D Journal of Automobile Engineering*, **2017**, 232: 1648-1653
16. Khalil, H., Hassan, H., Enhancement thermoelectric generators output power from heat recovery of chimneys by using flaps, *Elsevier Journal of Power Sources*, **2019**, 443: 227266
17. Lee, H., Attar, A.M., Weera, S.L., Performance prediction of commercial thermoelectric cooler modules using the effective material properties, *Journal of Electronic Materials*, **2015**, 44: 2157-2165
18. Attar, A., Lee, H., Weera, S.L., Experimental validation of the optimum design of an automotive air-to-air thermoelectric air conditioner (TEAC), *Journal of Electronic Mater*, **2015**, 44: 2177-2185
19. Snyder, G.J., Toberer, E.C., Complex thermoelectric materials, *Nature Materials*, **2008**, 7: 105-114
20. Goldsmid, H.J., *Introduction to thermoelectricity*, Berlin Heidelberg: Springer, **2010**
21. Lee, H.S., *Thermoelectrics design and materials*, USA: John Wiley, **2016**
22. Dhoopagunta, S., Analytical modeling and numerical simulation of a thermoelectric generator including contact resistances. Master's Theses, Western Michigan University, USA: **2016**
23. Li, Z., Li, W., Chen, Z., Performance analysis of thermoelectric based automotive waste heat recovery system with nanofluid coolant, *Energies*, **2017**, 10: 1489-1504
24. Nesarajah, M., Frey, G., Thermoelectric power generation: peltier element versus thermoelectric generator, In: *Iecon annual conference of the IEEE industrial electronics society*, Italy: 23-26 Oct. **2016**, 4252-4257
25. Incropera, F.P., DeWitt, D.P., *Fundamentals of heat and mass transfer*, USA: John Wiley & Sons, **2003**
26. Orak, I.M., Çelik, A.A., Parallel algorithm for defect detection of rail and profile in the manufacturing, *Journal of the Faculty of Engineering and Architecture of Gazi University*, **2017**, 32: 439-448
27. Yu, S., Du, O., Diao, H., Shu, G., Jiao, K., Start-up modes of thermoelectric generator based on vehicle exhaust waste heat recovery, *Applied Energy*, **2015**, 138: 276-290